Superior Stable and Long Life Sodium Metal Anodes Achieved by Atomic Layer Deposition

*Yang Zhao, Lyudmila V. Goncharova, Andrew Lushington, Qian Sun, Hossein Yadegari, Biqiong Wang, Wei Xiao, Ruying Li, and Xueliang Sun**

Na-metal batteries are considered as the promising alternative candidate for Li-ion battery beneficial from the wide availability and low cost of sodium, high theoretical specific capacity, and high energy density based on the plating/stripping processes and lowest electrochemical potential. For Na-metal batteries, the crucial problem on metallic Na is one of the biggest challenges. Mossy or dendritic growth of Na occurs in the repetitive Na stripping/plating process with an unstable solid electrolyte interphase layer of nonuniform ionic flux, which can not only lead to the low Coulombic efficiency, but also can create short circuit risks, resulting in possible burning or explosion. In this communication, the atomic layer deposition of Al_2O_3 coating is first demonstrated for the protection of metallic Na anode for Na-metal batteries. By protecting Na foil with ultrathin Al_2O_3 layer, the dendrites and mossy Na formation have been effectively suppressed and lifetime has been significantly improved. Furthermore, the thickness of protective layer has been further optimized with 25 cycles of Al_2O_3 layer presenting the best performance over 500 cycles. The novel design of atomic layer deposition protected metal Na anode may bring in new opportunities to the realization of the next-generation high energy-density Na metal batteries.

In the past several decades, Li-ion batteries (LIBs) become one of the most widely used energy storage device for portable electronic and electrical vehicles due to their superior features, including high energy density, no memory effect, low maintenance, and little self-discharge.[1] However, the limited resources and uneven distribution of lithium source become a serious challenge for low cost and large-scale application of LIBs.[2] The requirements for high-energy and low-cost rechargeable batteries have prompted the replacement of new battery system with conventional LIBs.[2,3] Na-ion batteries and Na-metal batteries are considered as a promising alternative candidate due to the wide availability and low cost of sodium.[4] Compared with other anodes used in Na-ion batteries, Na metal anode shows a high theoretical specific capacity of 1166 mAh g^{-1} based on the repeated plating/stripping processes and lowest electrochemical potential.[5] Meanwhile, the typical Na-metal batteries, including room temperature Na–S batteries and Na–O_2 batteries, both have a superior theoretical specific energy density (1274 Wh kg^{-1} for room temperature Na–S system and 1605 Wh kg^{-1} if considering Na_2O_2 as discharge product for Na–O_2 batteries, respectively) compared to Li-ion battery systems.[5,6]

For these room-temperature Na-metal batteries, main efforts are focusing on the design and fabrication of cathode electrode, however, the crucial problems on metallic Na anode still remain. Similar with Li metal anode: metallic Na reacts with most organic solvents in the liquid electrolyte leading to the formation of solid electrolyte interphase (SEI) layer upon directly contacting and also during the initial charge/discharge processes. The uniform and compact SEI layer effectively prevents the further physical contact between metallic Na and electrolyte, making Na dynamically stable in certain organic solvents. However, mossy or dendritic growth of Na will occur in the repetitive Na stripping/plating process with an unstable SEI layer of nonuniform ionic flux. Dendritic structures are unfavored because they not only lead to the low Coulombic efficiency but also can create short circuit risks when it ultimately penetrates the separator, reaching cathode electrode, further resulting in possible burning or explosion (**Figure 1**). Hartmann et al. observed the undesired growth of Na dendrites during cycling in the Na–O_2 batteries.[7] The hilly structure of Na dendrite composed of sodium and oxygen can also be found in the holes of separator. Another group also visually investigated the Na dendrite structure in Na–O_2 cell under various discharge capacity cut-off values.[8] Their results all demonstrate that the metallic Na anode is also a serious challenge affecting the performances and lifetime of Na–O_2 batteries beyond cathode electrode.

To data, there are only few reports exploring electrochemical plating/stripping of Na metal at room temperature.[9] Recently, Seh et al. have first reported that one type of liquid electrolyte, consisting of sodium hexafluorophosphate in glymes (mono-, di-, and tetraglyme), can enable highly reversible and

Y. Zhao, A. Lushington, Dr. Q. Sun, Dr. H. Yadegari, B. Q. Wang, W. Xiao, R. Li, Prof. X. Sun
Department of Mechanical and Materials Engineering
University of Western Ontario
London, Ontario N6A 5B9, Canada
E-mail: xsun@eng.uwo.ca
Prof. L. V. Goncharova
Department of Physics and Astronomy
University of Western Ontario
London, Ontario N6A 3K7, Canada

DOI: 10.1002/adma.201606663

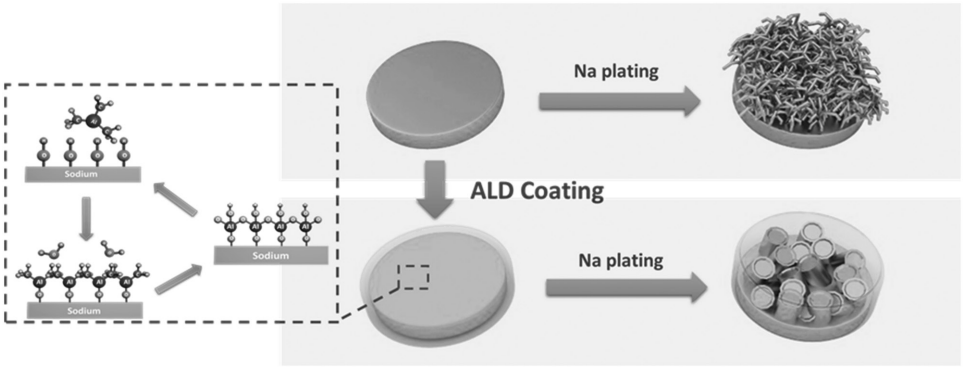

Figure 1. Schematic diagrams of Na stripping/plating on bare Na foil and Na foil with ALD coating.

nondendritic plating/stripping of sodium metal anodes at room temperature.[5] However, it is still believed that the mechanical strength of these in situ formed protective films by adjusting electrolyte is not yet high enough to withstand the large volume change during the process of Na plating/stripping.[10] Meanwhile, the physical cohesion of these thin films onto Na metal is very limited.[11] Moreover, especially for Na-O_2 batteries, the corrosion of Na metal under O_2 atmosphere can be another issue for the long cycle of cells.

In the previous study on Li metal batteries, the rational design of ex situ protective coating layers are widely accepted for reducing dendrite growth and suppressing O_2 corrosion.[12] The excessively sensitivity and quite low melting point of Na make it difficult to apply the general methods to deposit protective coating layer on the surface of Na metal. Atomic layer deposition (ALD) is a unique technique that can realize excellent coverage and conformal deposition and the thickness of the film deposited by ALD is precisely controllable at the nanoscale level due to its self-limiting nature.[13] A promising feature of ALD is the ability to conformably coat a surface at relatively low temperatures, which can enable the deposition of metals on Na metal, which has a low melting point of 98 °C. Our previous work has indicated that an ALD coating layer on the cathode and/or anode material for LIBs prevents direct contact of the electrolyte with the electrode, resulting in the formation of a stable SEI layer thereby increasing the electrochemical performance of the LIBs.[14] Recently, two different groups have demonstrated ultrathin ALD Al_2O_3 coating film as protective layer for lithium metal anode. Their results indicate that ALD protective coating layer can effectively prevent Li metal corrosion in electrolyte and reduce the dendrite growth as well further enhancing electrochemical performances with higher capacity and longer lifetimes.[15,16] It is also considered that ALD Al_2O_3 can be a promising candidate for Na protection due to the following reasons. (1) The low reaction temperature of ALD Al_2O_3 can be deposited within an acceptable temperature range. (2) With electrochemical cycling, Al_2O_3 will form $NaAlO_x$, which has demonstrated high ionic conductivity.[17]

In this communication, we demonstrated the successful application of the ALD technique to create an ultrathin protective coating on Na metal anode to achieve long lifetime Na metal batteries. Here, it should be mentioned that, after the initial submission of the present communication, Luo et al. reported a plasma-ALD process of Al_2O_3 for Na anode protection.[18] However, our work here reveals more comprehensive study on electrochemical performances and relationship between plating/stripping properties and morphologies. Moreover, we also discuss the detailed reaction mechanisms by advanced characterization techniques such as Rutherford backscattering spectrometry (RBS) and X-ray photoelectron spectroscopy (XPS). To the best of our knowledge, we are the first to demonstrate a powerful tool of RBS measurement in the field of Li or Na metal anode, which give a guidance to the researchers working in this area.

Compared with bare Na foil, the ALD-coated Na presents significantly enhanced Na plating/stripping performance. Furthermore, the ALD Al_2O_3 coating thickness has also been optimized in detail. The glovebox-integrated ALD tool was used in this work to directly deposit Al_2O_3 coating layer on Na metal without any air exposure. The typical ALD Al_2O_3 coating process is shown in Figure 1a with two half reactions between trimethylaluminum (TMA) and H_2O. Based on the growth rate of Al_2O_3 under low temperature, the thickness of 10, 25, and 50 cycles of ALD Al_2O_3 can be defined as 1.4, 3.5, and 7 nm, respectively.

Galvanostatic cycling performance of Na with ALD Al_2O_3 coating layers and bare Na foil were studied in a symmetrical cell configuration using 1 M $NaSO_3CF_3$ dissolved in diethylene glycol dimethyl ether. **Figure 2**a shows the cycling stability of Na coated with 25 cycles of Al_2O_3 by ALD (Na@25Al_2O_3) and the bare Na foil at a current density of 3 mA cm^{-2} with a capacity limitation of 1 mAh cm^{-2}. For the bare Na foil, the initial Na stripping/plating overpotential is about 20 mV (vs Na^+/Na), and rapidly increases to over 50 mV (vs Na^+/Na) after 100 cycles (equal to 100 h). Meanwhile, obvious fluctuating voltage profiles during Na stripping/plating process can be observed, with soft short circuiting of the cell occurring after 50 cycles (equal to 50 h). Interestingly, Na@25Al_2O_3 demonstrates a similar initial overpotential of about 20 mV (vs Na^+/Na), but a very negligible change in overpotential following 100 cycles (17 mV vs Na^+/Na) (equal to 100 h). Detailed voltage profiles of Na@25Al_2O_3 and bare Na foil after the first cycle and following 100 cycles are shown in Figure 2b,c. For Na@25Al_2O_3, a flat voltage plateau at both the charging and discharging states can be retained throughout the whole cycle without obvious increases in hysteresis. Meanwhile, it can also be noticed that due to the extremely sensitive and highly reducibility of Na metal anode, there is unstable change in the voltage profiles at the first cycle, which can be explained as the formation of

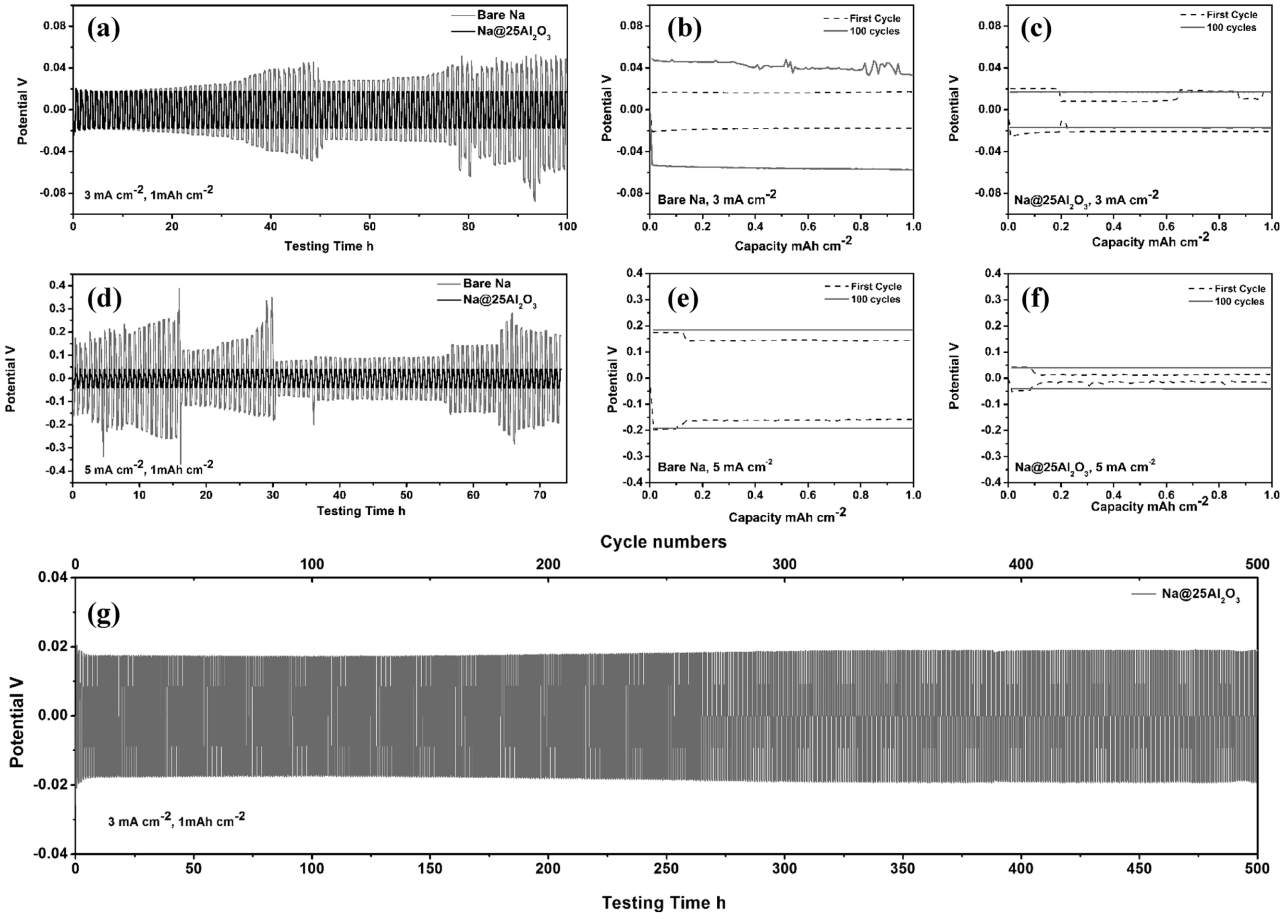

Figure 2. a) Comparison of the cycling stability of the Na@25Al_2O_3 and the bare Na foil at a current density of 3 mA cm^{-2}. b,c) Voltage profiles of Na@25Al_2O_3 and bare Na foil in the first cycles and after 100 cycles at a current density of 3 mA cm^{-2}. d) Comparison of the cycling stability of the Na@25Al_2O_3 and the bare Na foil at a current density of 5 mA cm^{-2}. e,f) Voltage profiles of Na@25Al_2O_3 and bare Na foil in the first cycles and after 100 cycles at a current density of 5 mA cm^{-2}. The amount of Na cycled was 1 mAh cm^{-2}. g) Long cycle life of Na@25Al_2O_3 at 3 mA cm^{-2}.

initial SEI film due to the reaction between surface of Na anode (coated and uncoated) and electrolyte. When increasing current density to 5 mA cm^{-2}, the initial Na stripping/plating overpotential increases to 160 mV (vs Na^+/Na) with the highest overpotential exceeding 300 mV during cycling (Figure 2d). Meanwhile, after only 21 cycles (equal to 17 h), a sudden drop of voltage can be observed for the bare Na with fluctuating voltage in the following cycles, which could be explained as a soft short circuit occurring within the cell as a result of Na dendrite penetration. It can be found that the lifetime of bare Na is shortened with increasing current density. However, with 25 cycles of ALD Al_2O_3 coating, the modified Na foil demonstrates reduced lower initial overpotential (38 mV vs Na^+/Na), which is extremely stable after 100 cycles with the overpotential of 40 mV (vs Na^+/Na). In order to show the convinced performances from ALD Al_2O_3-coated Na anode, higher current density (10 mA cm^{-2}) is applied, which is shown in Figure S1 (Supporting Information). From the results, the Na@25Al_2O_3 indicates superior stable plating/stripping performances after 150 cycles (equal to 80 h), which is much better than bare Na foil.

To further explain the performances, electrochemical impedance spectroscopy (EIS) was performed at the point before cycling and after 50 cycles, as shown in Figure S5 (Supporting Information). It is believed that two distinct semicircles are associated with both the SEI/electrode (high frequency) and the charge transfer/electrical double layer (lower frequencies).[16] Impedance parameters calculated by equivalent circuits for different samples are shown in Table S1 (Supporting Information). The initial spectra in Figure S5a (Supporting Information) indicate a slight increase in the impedance for the Na@25Al_2O_3 compared with bare Na foil before cycling. After 50 cycles of plating/stripping process, R_{SEI} of bare Na showing an obvious increase, however, Na@25Al_2O_3 indicating a decrease. Meanwhile, the R_{SEI} of Na@25Al_2O_3 becomes smaller than the bare Na foil, which can be attributed to the stable SEI layer with 25 cycles Al_2O_3 coating.

To optimize the thickness of the ALD protective layer on the stripping/plating performance of Na metal, various cycles of ALD Al_2O_3 (10 and 50 cycles) are applied to achieve the controllable thickness of Al_2O_3 layer on Na metal. Compared with bare Na, both Na@10Al_2O_3 and Na@50Al_2O_3 have the significant improvement with lower overpotential and enhanced stability (Figures S2 and S3, Supporting Information). However, a thinner coating of 10 cycles ALD Al_2O_3, voltage fluctuations

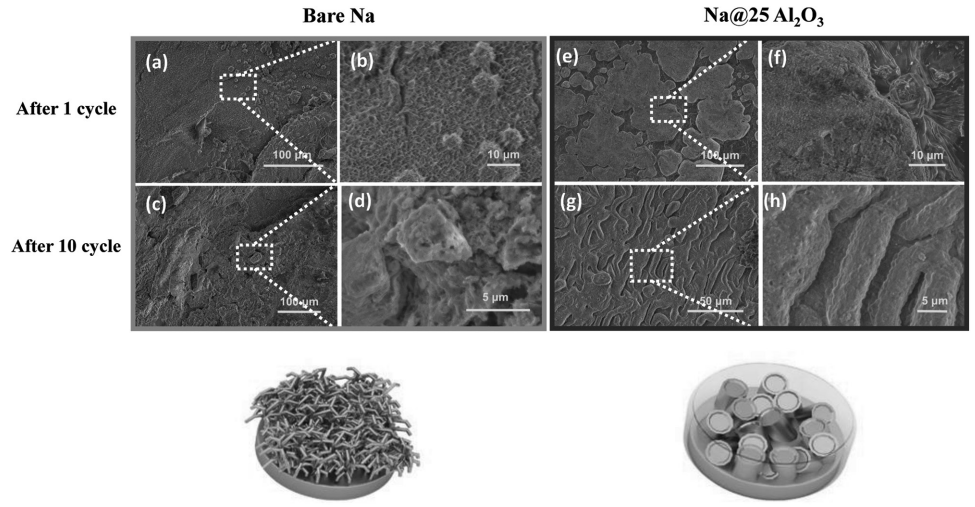

Figure 3. Top-view SEM images of a,b) bare Na and e,f) Na@25Al_2O_3 after 1 cycle of stripping/plating and c,d) bare Na and g,h) Na@25Al_2O_3 after 10 cycles of stripping/plating at a current density of 3 mA cm^{-2}.

begin to appear at around 80 cycles (equal to 80 h) with a current density of 3 mA cm^{-2} (Figure S2a, Supporting Information). Increasing the current density to 5 mA cm^{-2}, the Na/Al_2O_3-10 demonstrates an obvious continuous rise in hysteresis (Figure S3a, Supporting Information). Similar results can be obtained with thicker coating of 50 cycles of ALD Al_2O_3. Although enhanced stability can be achieved, the modified Na foil with 50 cycles Al_2O_3 protective layers still shows the higher overpotential and increasing hysteresis compared with 25 cycles ALD Al_2O_3 coating (Figures S2b and S3b, Supporting Information). The EIS results (as shown in Figure S5a,b and Table S1 in the Supporting Information) also give consistent evidence with the electrochemical performances. For the thinner coating of 10 cycles Al_2O_3, the R_{SEI} shows an obvious decrease after 50 cycles, which is even smaller than bare Na. However, the Na@50 Al_2O_3 demonstrates the increasing of R_{SEI} after 50 cycles of plating/stripping, confirming the increasing resistance and hysteresis compared with bare Na and Na@25 Al_2O_3. Thus, it is very important to optimize the thickness of Al_2O_3 for protect Na. The EIS results indicate the significantly reduced degradation during cycling of optimized thickness of Al_2O_3 coating, leading to lower resistance and increase of lifetime.

With the optimized thickness of ALD Al_2O_3 coating layer (25 cycles), the modified Na foil shows superior stripping/plating performances with superlong lifetime. Even after 500 cycles, there is almost no change in the Na stripping/plating behavior (Figure 2g). The flat charging and discharging voltage plateau can also be obtained with different stripping/plating cycles of 200, 250, 300, 350, 400 in the detailed voltage profiles at the current density of 3 mA cm^{-2} (Figure S4, Supporting Information).

In order to understand the influence of ALD Al_2O_3 coating on the morphologies of Na plating/stripping, the scanning electron microscopy (SEM) images of the electrodes before and after cycling were analyzed by SEM. Microscopy of the bare Na foil surface is shown in Figure S6 (Supporting Information). Following 25 cycles of ALD Al_2O_3 coating (Figure S6, Supporting Information), there is no obvious difference of the quite smooth surface due to the ultrathin thickness of coating layers. When a capacity limitation of 1 mAh cm^{-2} was used along with a current density of 3 mA cm^{-2}, two type of Na structures can be observed on the surface, moss-like Na (**Figure 3**a,b) and dendritic Na (Figure S7, Supporting Information). For the moss-like Na shown in Figure 3a,b, the sphere-like structure of Na with the sizes about 5 μm can be observed which is forming with the moss-like dendrites under nanoscale. More rough structure with dendritic Na can also be found in the top view SEM images (Figure S7, Supporting Information), which shows the large diameter of a few microns. These types of moss/dendritic Na will further lead to the formation of dead sodium during the plating/stripping process, which will consume effective Na and lower the Columbic efficiency. Very interestingly, with ALD Al_2O_3 coating, the morphologies of the plating Na are totally changed compared with bare Na foil. Figure 3e,f shows the SEM images of Na@25Al_2O_3 after 1 cycle of stripping/plating under the current density of 3 mA cm^{-2}. With ALD Al_2O_3 coating, large island-like Na is produced with a diameter of over 100 μm, in which the surface of the Na island is smoother without any moss-like and/or dendritic Na. The plating behavior of bare and modified Na after 10 cycles has also been studied. After 10 cycles, the bare Na suffers from the serious destruction with the appearance of a rough surface littered with cracks (as shown in Figure 3c,d). However, with 25 cycles of ALD coating, the island-like Na is still stable after 10 cycles of the stripping/plating process. This demonstrates that island-like Na structures can be well maintained during the cycling compared with the moss-like and dendritic Na (as shown in Figure 3g,h). Increasing the current density to 5 mA cm^{-2}, more out-of-flatness surface with even big cracks can be seen for the bare Na after 1 cycle plating process (Figure S10, Supporting Information). However, with 25 cycles of ALD Al_2O_3, the island-like Na can still be achieved with a flat surface at a high current density of 5 mA cm^{-2} (Figure S12, Supporting Information). Meanwhile, the SEM images of Na with 10 and 50 cycles of ALD Al_2O_3 coating have also been tested under different current densities (3 and 5 mA cm^{-2}). It can be found

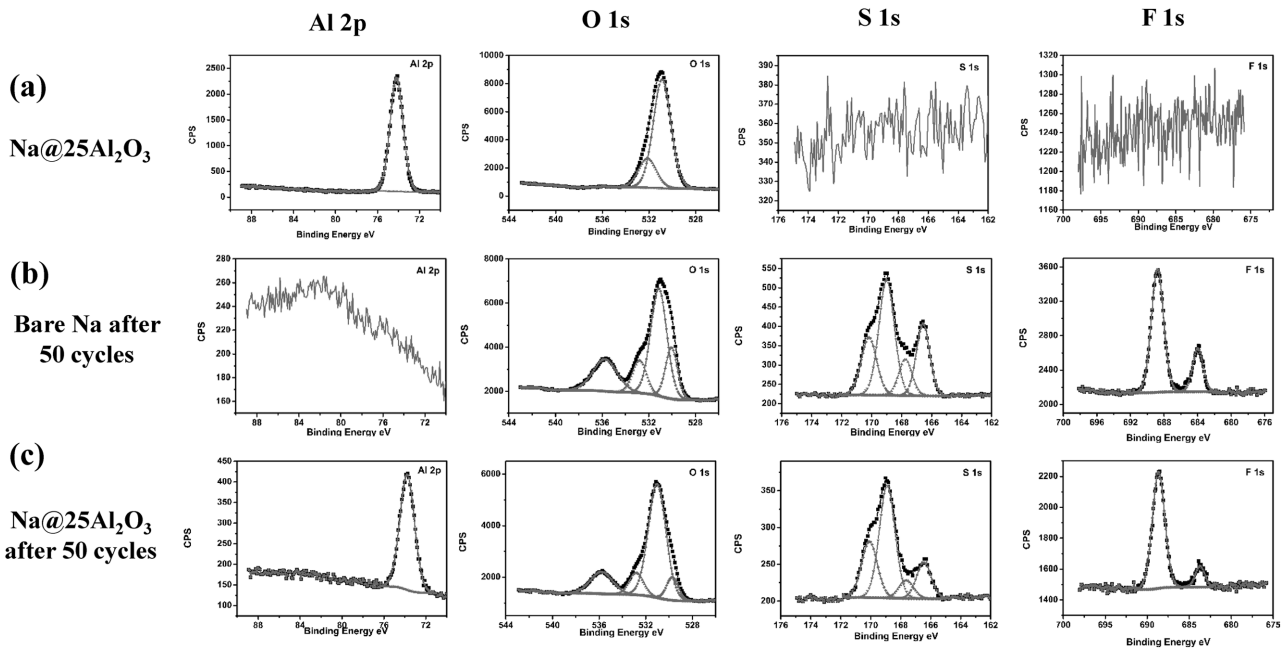

Figure 4. XPS Al 2p, O 1s, S 1s, and F 1s spectrum of a) Na-Al_2O_3 25, b) bare Na, and c) Na-Al_2O_3 25 after 50 cycles of plating/stripping at the current density of 3 mA cm^{-2}.

that with the assistance Al_2O_3 coating, the Na dendrite can be effectively inhibited to form the island-like structure, which can play an important role in the improved electrochemical performance (Figures S8–S13, Supporting Information). The grown of island-like structure on the surface of Na can be attributed to the very uniform and dense Al_2O_3 coating layer, leading to even distribution of the electric field and further as the large and island-like Na growth.

XPS testing was employed to determine the chemical nature of the Na surface before and after plating/stripping process (Table S2, Supporting Information). Figure S14 (Supporting Information) shows the XPS spectra of Na foil with 25 cycles Al_2O_3, bare Na, and Na@25Al_2O_3 after 50 cycles of plating/stripping. From the spectra of Na@25Al_2O_3 before cycling, the peaks of Al 2p and Al 2s at 74.18 and 116.35 eV demonstrate the successful deposition of Al_2O_3 on the surface of Na foil by ALD. The Na 1s spectra of all samples have been presented in Figure S15 (Supporting Information), which is mainly from the metal Na on the surface of the samples. The detailed XPS spectrum of Al 2p, O 1s, S 1s, and F 1s for each sample is shown in **Figure 4**. Bare Na foil after 50 cycles of plating/stripping results in the formation of an SEI composed of organic products including RCH_2ONa (O 1s at 532.79 eV) and inorganic products of Na_2O (O 1s at 530.05 eV), NaF (F 1s at 683.99 eV), Na_2SO_3 and Na_2SO_4 (O 1s at 531.14 eV and S 2p at 164–172 eV).[5] Though very promising, the Al_2O_3 protective layers can still remain after 50 cycles of plating/stripping (Figure 4c), demonstrating the stable properties of Al_2O_3 as an artificial SEI film on the surface. Meanwhile, from the spectrum of O 1s and F 1s, the contents of RCH_2ONa, Na_2O, and NaF have been effectively decreased, which declares the less reaction and reduction between the electrolyte and Na foil with the protection of Al_2O_3 coating. More evidence can be found from the spectrum of S 1s, more Na_2SO_4 exists with Al_2O_3 coatings, preventing its reduction into Na_2SO_3. It is considered that the less uniform SEI film of $NaSO_3CF_3$ in DEMDME causes more Na exposing to undesirable side reactions with electrolyte, forming more organic reduction products in the SEI and lowering the Coulombic efficiency.[5] However, the Al_2O_3 coating layers can act as the artificial SEI film with electrochemical stable properties during plating/stripping and effectively reduce the reaction between Na anode and electrolyte to form a more stable SEI layer resulting in preventing the Na dendrite growth and improved lifetime.

RBS measurements were performed on Al_2O_3-coated Na (before cycling), bare Na, and Al_2O_3-coated Na after 50 cycles. Figure S16 (Supporting Information) shows that as-deposited Al_2O_3 film forms continuous layer ≈12 nm thick, assuming Al_2O_3 density of 2.7 g cm^{-3}. Absences of surface Na peak indicate that there are no voids in Al_2O_3 layer. Experimental ion yields are best fitted assuming formation of intermixed ≈10 nm thick Al_2O_3-Na_2O oxide layer. RBS spectra and calculated depth profiles for samples after cycling are presented in **Figure 5**. Both Al_2O_3-coated and bare Na samples exhibited S peaks due to the interactions with electrolyte during cycling. Al peak is clearly visible in Al_2O_3-coated Na sample after cycling; however, Al has a wider depth distribution as it is intermixed with Na–S–O phase. From integrated areal densities for Al peak before and after cycling we estimate that ≈85 ± 5% of as-deposited Al remains on the surface. Amount of S is consistent with our XPS results on similar samples (Figure 4). S areal density is a factor of two larger for bare Na sample compared to Al_2O_3-coated Na.

The significant improvement on the electrochemical performances of ALD-coated Na electrode can be attributed to the suppressed dendrite growth assistant with ultrathin ALD Al_2O_3

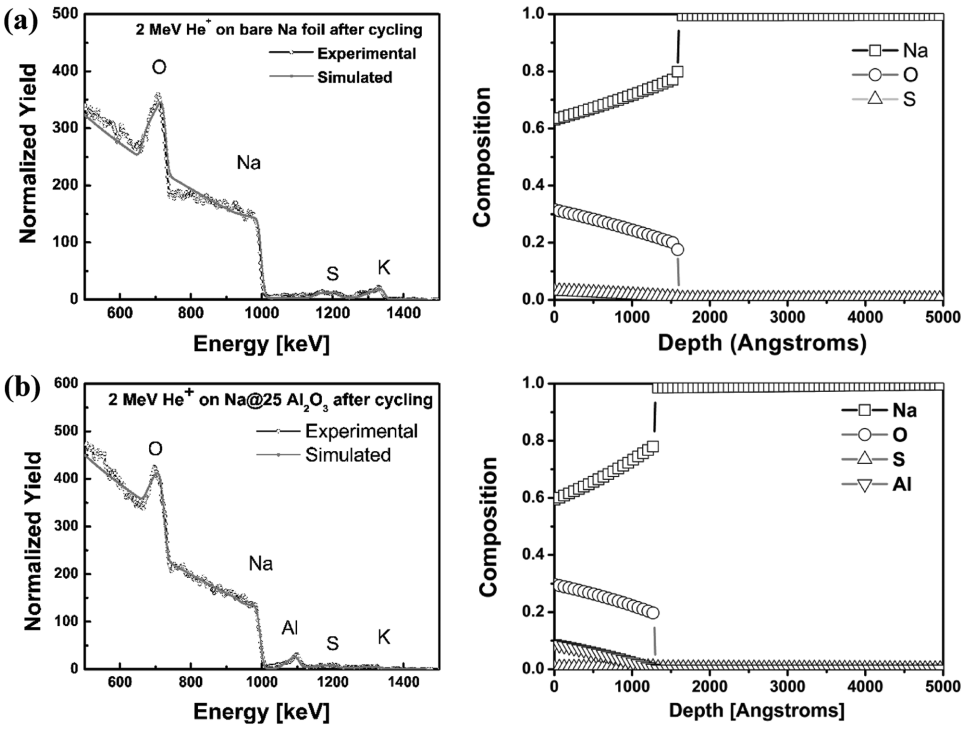

Figure 5. RBS spectra and calculated depth profiles of bare Na and Na-Al_2O_3 25 after 50 cycles of plating/stripping at the current density of 3 mA cm^{-2}.

protective coating layer. Obviously, both the initial cycle and 100 cycles overpotential of Na stripping/plating is much smaller for the Al_2O_3-coated Na foil, especially at high current densities (Figure 2), which indicates the lower interfacial charge transfer resistance. Meanwhile, the smooth stripping/plating voltage profile of Al_2O_3-coated Na foil can also reduce local current density, which further results in the flat and smooth surface of the island-like Na formation during plating/stripping process. Furthermore, with the artificial Al_2O_3 coating layers, the side reaction between Na and electrolyte can be effectively reduced to form a stable SEI film. As a result, the modified Na anode can achieve very stable plating/stripping performances under very high current density with superior long lifetime over 500 h.

In conclusion, we have successfully demonstrated the concept of ALD Al_2O_3 protective coating on metallic Na foil for long life Na metal batteries for the first time. By protecting Na foil with ultrathin Al_2O_3 layer, the dendrites and mossy Na formation have been effectively suppressed and lifetime has been significantly improved. Based on the plating/stripping tests, the thickness of protective layer has been further optimized, in which 25 cycles of Al_2O_3 layer indicating the best performance as well as superior long and stable lifetime over 500 cycles. The presented design of ALD Al_2O_3-coated metal Na anode may bring in new opportunities to the realization of the next-generation high energy-density Na metal batteries.

Experimental Section

Electrode Preparation: A fresh Na foil with the diameter of 7/16 in. was prepared with the aid of a homemade press machine by pressing a piece of sodium metal stick (from Aldrich) as a starting sodium metal inside an argon-filed glove box. ALD coatings were conducted on Na foils in a Gemstar-8 ALD system (Arradiance, USA) which was directly connected to an argon-filed glove box. Al_2O_3 was directly deposited on the Na foil at 85 °C by using TMA and water (H_2O) as precursors. The different cycle numbers of 10, 25, and 50 ALD Al_2O_3 coating on Na metal are named as Na@10Al_2O_3, Na@25Al_2O_3, and Na@50Al_2O_3, respectively.

Electrochemical Measurements: The electrochemical analysis was performed in CR2032 coin-type cells. The coin cells were assembled in an ultrapure argon-filled glove box by symmetrical Na/electrolyte-separator/Na configuration using polypropylene separators (Celgard 3501). The electrolyte used in this study is 1 M sodium triflate ($NaSO_3CF_3$ 98%, Aldrich) dissolved in diethylene glycol dimethyl ether (reagent grade ≈98%, Aldrich, predried before usage), which has been also used in our group for Na–O_2 studies.[6] The Na stripping/plating studies were carried out in an Arbin BT-2000 Battery Test System at room temperature. Constant current densities were applied to the electrodes during repeated stripping/plating while the potential was recorded over time. EIS was also performed on the versatile multichannel potentiostat 3/Z (VMP3).

Characterization: SEM images were taken using a Hitachi 3400N environmental scanning electron microscopy at an acceleration voltage of 5 kV. Due to the soft properties of Na metal, Swagelok-type cells comprised of Na/electrolyte-separator/Na system were used to carry out the morphology testing after stripping/plating. The Swagelok cells were disassembled after 1 cycle or 10 cycles of stripping/plating process under the different current densities. The Na foil and Na@25Al_2O_3 (before and after plating/stripping) were transferred from our ALD glove box directly to an Ar glove box connected XPS (Kratos AXIS Ultra Spectrometer) system for XPS analysis. Rutherford backscattering spectrometry measurements were conducted using 1 and 2 MeV He^+ beam (Western Tandetron Facility) at several locations on the surface to confirm the uniformity of the thicknesses and composition. All samples were transferred in Ar-filled glove bag with minimum exposure to air. An Sb-implanted amorphous Si sample with a known 4.82×10^{15} atoms cm^{-2} Sb content was used for calibration.

Supporting Information

Supporting Information is available from the Wiley Online Library or from the author.

Acknowledgements

This research was supported by the Natural Science and Engineering Research Council of Canada (NSERC), the Canada Research Chair Program (CRC), the Canada Foundation for Innovation (CFI), and the University of Western Ontario (UWO).

Received: December 8, 2016
Published online: March 3, 2017

[1] a) Y. Zhao, X. Li, B. Yan, D. Xiong, D. Li, S. Lawes, X. Sun, *Adv. Energy Mater.* **2016**, *6*, 1502175; b) Y. Zhao, X. Li, B. Yan, D. Li, S. Lawes, X. Sun, *J. Power Sources* **2015**, *274*, 869.
[2] V. Palomares, P. Serras, I. Villaluenga, K. B. Hueso, J. Carretero-González, T. Rojo, *Energy Environ. Sci.* **2012**, *5*, 5884.
[3] a) K. B. Hueso, M. Armand, T. Rojo, *Energy Environ. Sci.* **2013**, *6*, 734; b) X. Lu, B. W. Kirby, W. Xu, G. Li, J. Y. Kim, J. P. Lemmon, V. L. Sprenkle, Z. Yang, *Energy Environ. Sci.* **2013**, *6*, 299.
[4] a) M. D. Slater, D. Kim, E. Lee, C. S. Johnson, *Adv. Funct. Mater.* **2013**, *23*, 947; b) V. Palomares, M. Casas-Cabanas, E. Castillo-Martínez, M. H. Han, T. Rojo, *Energy Environ. Sci.* **2013**, *6*, 2312.
[5] Z. W. Seh, J. Sun, Y. Sun, Y. Cui, *ACS Cent. Sci.* **2015**, *1*, 449.
[6] a) H. Yadegari, Y. Li, M. N. Banis, X. Li, B. Wang, Q. Sun, R. Li, T.-K. Sham, X. Cui, X. Sun, *Energy Environ. Sci.* **2014**, *7*, 3747; b) Q. Sun, H. Yadegari, M. N. Banis, J. Liu, B. Xiao, B. Wang, S. Lawes, X. Li, R. Li, X. Sun, *Nano Energy* **2015**, *12*, 698; c) H. Yadegari, M. N. Banis, B. Xiao, Q. Sun, X. Li, A. Lushington, B. Wang, R. Li, T.-K. Sham, X. Cui, X. Sun, *Chem. Mater.* **2015**, *27*, 3040; d) Q. Sun, H. Yadegari, M. N. Banis, J. Liu, B. Xiao, X. Li, C. Langford, R. Li, X. Sun, *J. Phys. Chem. C* **2015**, *119*, 13433.
[7] P. Hartmann, C. L. Bender, J. Sann, A. K. Durr, M. Jansen, J. Janek, P. Adelhelm, *PCCP Phys. Chem. Chem. Phys.* **2013**, *15*, 11661.
[8] N. Zhao, C. Li, X. Guo, *PCCP Phys. Chem. Chem. Phys.* **2014**, *16*, 15646.
[9] a) J. S. W. Thomas, L. Riechel, *J. Electrochem. Soc.* **1992**, *139*, 977; b) R. A. O. J. Fuller, *J. Electrochem. Soc.* **1995**, *142*, 3632; c) P. A. K. Gary, E. Gray, J. Winnick, *J. Electrochem. Soc.* **1995**, *142*, 3636; d) B. J. Piersma, *J. Electrochem. Soc.* **1996**, *143*, 908; e) R. Wibowo, L. Aldous, E. I. Rogers, S. E. W. Jones, R. G. Compton, *J. Phys. Chem. C* **2010**, *114*, 3618; f) S. H. Park, J. Winnick, P. A. Kohl, *J. Electrochem. Soc.* **2001**, *148*, A346.
[10] Z. Liang, G. Zheng, C. Liu, N. Liu, W. Li, K. Yan, H. Yao, P. C. Hsu, S. Chu, Y. Cui, *Nano Lett.* **2015**, *15*, 2910.
[11] K. Yan, H. W. Lee, T. Gao, G. Zheng, H. Yao, H. Wang, Z. Lu, Y. Zhou, Z. Liang, Z. Liu, S. Chu, Y. Cui, *Nano Lett.* **2014**, *14*, 6016.
[12] a) G. Zheng, S. W. Lee, Z. Liang, H. W. Lee, K. Yan, H. Yao, H. Wang, W. Li, S. Chu, Y. Cui, *Nat. Nanotechnol.* **2014**, *9*, 618; b) D. J. Lee, H. Lee, Y.-J. Kim, J.-K. Park, H.-T. Kim, *Adv. Mater.* **2016**, *28*, 857; c) C. B. Bucur, A. Lita, N. Osada, J. Muldoon, *Energy Environ. Sci.* **2016**, *9*, 112; d) H. Lee, D. J. Lee, Y.-J. Kim, J.-K. Park, H.-T. Kim, *J. Power Sources* **2015**, *284*, 103.
[13] a) X. Meng, X. Q. Yang, X. Sun, *Adv. Mater.* **2012**, *24*, 3589; b) J. Liu, X. Sun, *Nanotechnology* **2015**, *26*, 024001.
[14] a) X. Li, J. Liu, M. N. Banis, A. Lushington, R. Li, M. Cai, X. Sun, *Energy Environ. Sci.* **2014**, *7*, 768; b) X. Li, J. Liu, B. Wang, M. N. Banis, B. Xiao, R. Li, T.-K. Sham, X. Sun, *RSC Adv.* **2014**, *4*, 27126; c) X. Li, A. Lushington, J. Liu, R. Li, X. Sun, *Chem. Commun.* **2014**, *50*, 9757; d) B. Xiao, J. Liu, Q. Sun, B. Wang, M. N. Banis, D. Zhao, Z. Wang, R. Li, X. Cui, T.-K. Sham, X. Sun, *Adv. Sci.* **2015**, *2*, 1500022.
[15] A. C. Kozen, C.-F. Lin, A. J. Pearse, M. A. Schroeder, X. Han, L. Hu, S.-B. Lee, G. W. Rubloff, M. Noked, *ACS Nano* **2015**, *9*, 5884.
[16] E. Kazyak, K. N. Wood, N. P. Dasgupta, *Chem. Mater.* **2015**, *27*, 6457.
[17] S. C. Jung, H. J. Kim, J. W. Choi, Y. K. Han, *Nano Lett.* **2014**, *14*, 6559.
[18] W. Luo, C. F. Lin, O. Zhao, M. Noked, Y. Zhang, G. W. Rubloff, L. B. Hu, *Adv. Energy Mater.* **2016**, 1601526.